



ISSN: 0067-2904

## Simulation of Obstacle Avoidance for Auto Guided Land Vehicle

Laith A. Al-Ani<sup>1</sup>, Mohammed Sahib Mahdi Altaei<sup>2</sup>, Qudama Khamees<sup>\*3</sup>

<sup>1</sup>Department of Physics, College of Science, Al-Nahrain University, Baghdad, Iraq

<sup>2</sup>Department of Computers, College of Science, Al-Nahrain University, Baghdad, Iraq

<sup>3</sup>Department of Physics, College of Science, University of Anbar, Anbar, Iraq

### Abstract

This research is concerned with designing and simulating an auto control system for a car provided with obstacle avoidance sensors. This car is able to pass through predefined path around the detected obstacles, and then come back to the intended path. The IR sensor detects the existence of the obstacle through an assumed range of detection, while the visual sensor (camera) feeds back an image including the path that contains an obstacle, which can be useful for determining the obstacle's length, speed, and direction. According to such information, the controller creates transient away point along the longitudinal axis of the obstacle which is the same as the transverse axis of the simulator path at an assumed distance from the obstacle. The robotic car will direct toward the transient point for avoiding the obstacle, which directly come back into the original route once when reaching the transient point. This strategy enables the car to move far away from the obstacle and then return it into planned path.

**Keywords:** IR sensor, Visual sensor, Obstacle avoidance, Mobile robot.

### محاكاة تجنب الموانع لمركبة أرضية ذاتية القيادة

ليث عبد العزيز العاني<sup>1</sup>، محمد صاحب الطائي<sup>2</sup>، قدامة خميس هذال<sup>\*3</sup>

<sup>1</sup>قسم الفيزياء، كلية العلوم، جامعة النهرين، بغداد، العراق

<sup>2</sup>قسم الحاسبات، كلية العلوم، جامعة النهرين، بغداد، العراق

<sup>3</sup>قسم الفيزياء، كلية العلوم، جامعة الأنبار، الأنبار، العراق

### الخلاصة

يتضمن هذا البحث تصميمًا وحاكي نظامًا للتحكم التلقائي في قيادة السيارة باستخدام مستشعرات تجنب العقبات. هذه السيارة قادرة على المرور عبر مسار محدد مسبقًا وتميرير حول العقبات التي تم الكشف عنها، ومن ثم العودة إلى المسار المقصود. يقوم مستشعر الأشعة تحت الحمراء بالكشف عن وجود العائق من خلال نطاق الكشف المفترض، بينما يقوم المستشعر البصري (الكاميرا) بإعادة تغذية الصورة بما في ذلك المسار الذي يحتوي على عقبة، والتي يمكن أن تكون مفيدة لتحديد طول العائق وسرعته واتجاهه. ووفقًا لمثل هذه المعلومات، فإن وحدة التحكم تخلق نقطة عابرة بعيدًا على طول المحور الطولي للعائق، وهو نفس المحور المقابل لمسار المحاكي، وبعيدًا عن العائق بمسافة أمان مفترضة. ستوجه السيارة الآلية نحو نقطة عابرة لتجنب العائق، والتي تعود مباشرة إلى المسار الأصلي مرة واحدة عند الوصول إلى نقطة عابرة. هذه الاستراتيجية تمكن السيارة من الانتقال بعيدًا عن العائق ومن ثم إعادته إلى المسار المخطط له.

\*Email: qudama Khamees@gmail.com

## Introduction

Navigation of a robot without external help is important aspects for developing functioning autonomous mobile robot. It also refers to the ability of the robot to determine its position in its environment and then to plan a path towards some goal location. Computer simulations are used widely as valuable design and testing tools [1, 2]. Navigation is a control system that focuses on the process of monitoring and controlling the movement of a vehicle from one place to another [3, 4]. Obstacle avoidance in robotics is the task of satisfying some control objective subject to non-intersection or non-collision position constraints. The analysis shows critical situations of obstacle avoidance according to the control concepts Obstacle avoidance is considered to be distinct from path planning in that one is usually implemented as a reactive control law while the other involves the pre-computation of obstacle free path which a controller will guide a robot along Darius B. et al in 2002 presented a stereo-based obstacle avoidance system for mobile vehicles. They model the surface geometry of supporting surface and removes the supporting surface from the scene. The remaining stereo disparities are segmented into connected components in image and disparity space. Then, the resulting connected components are used to plan a path around them. The algorithm developed has been implemented on a mobile robot equipped with a real time stereo system [5]. Kyuhyong Y. in 2008 presented autonomous navigation and obstacle avoidance vehicle. The concept of the designed robot depends on electronics and software to enable robots to do almost anything one can imagine and its boundary will be expanded. The objective is to design a car based robot that can navigate through geographical positioning system (GPS) coordinates automatically. The robot is based on regular radio controlled (RC) car and entire components including microprocessor and sensors are on the same base [6]. Taichi Y. in 2013 presented a method to closely follow the global designated path by setting manually. In which, the robot moves in a range of velocities and thus being able to avoid obstacle staying closely to the designated path. The results of the experiments verify that this method is able to let the robot move closely to the designated path while avoiding moving obstacle [7]. Anish Pandey in 2017 establishing a review article about mobile robot navigation and obstacle avoidance techniques, where the applications of the autonomous mobile robot in many fields such as industry, space, defense and transportation, and other social sectors are growing day by day. It focuses on the study of the intelligent navigation techniques, which are capable of navigating a mobile robot autonomously in static as well as dynamic environments [8].

This paper concerned with using a fast and flexible robotic guidance model for designing an auto-guided land vehicle is moving predefined path. The estimated vehicle velocities at any position (x,y) are fed into the controller during the navigation trip to estimate the amount of corrections for both the position and head of the vehicle. The successful simulation encourages extending the experiment to include obstacle avoidance problem. A novel fast and simple method is used to handle the obstacle avoidance is operated simultaneously with the guidance process.

### Robotic Guidance Model

The instantaneous car position is determined by the Cartesian coordinate system (or even ECS; *longitude* and *latitude*) via specific sensors. The geometrical description of the ECS is very difficult to use due to its curved imaginary lines along the Earth's surface. This difficulty is solved by adopting a simplified linear approximation rather than EMS, which can be applied on relatively small Earth region as follows[9]. :

$$\begin{bmatrix} X \\ Y \end{bmatrix} = \begin{bmatrix} Lat & 0 \\ 0 & Lon \end{bmatrix} \begin{bmatrix} X_o \\ Y_o \end{bmatrix} = \begin{bmatrix} Lon - Lon_o \\ Lat - Lat_o \end{bmatrix} \quad \dots (1)$$

where  $Lon_o$  and  $Lat_o$  represent the longitude and latitude respectively of the reference point which can be chosen as a midpoint within the planned guidance path. This transformation is valid only for a small geographical navigation region (such as Iraq). The 2-D space that determines the position of the car, is described by the two plane axes  $X$  and  $Y$  that determine the head of the car on the surface of the Earth with respect to reference point. The instantaneous components of the car's velocity could be described by the spherical coordinates as follows[10]. :

$$V_x = V \cos(\text{Head})$$

$$V_y \approx \frac{\Delta y}{\Delta t} = V \sin(\text{Head}) \quad \dots (2)$$

where,  $\Delta x$ , and  $\Delta y$  are the positioning deflections respectively during one short time interval  $\Delta t$ ,  $\text{Head}$  is the head angle of the car.

Equations (1) can be utilized to determine the positioning deflection due to the car motion, which leads to determine the deflections of the car head as follows[11]. :

$$\Delta \text{Head} = \tan^{-1}\left(\frac{\Delta x}{\Delta y}\right) \quad \dots (3)$$

where,  $\Delta \text{Head}$  is the deflection of the head.

### Guidance Parameters

Guidance parameters describe the guidance tools of the car and its relation with navigation parameters; they include the angular descriptors of the wheels rotation. When the car needs to be turned, the guidance parameter that is responsible for the turn is the wheel rotation ( $R$ ), which is determined by the range  $-45$  to  $45^\circ$  direction. Whilst, the guidance parameter that responsible on changing the speed is the revolution per minute ( $RPM$ ) of the car's engine as shown in Figure-1.

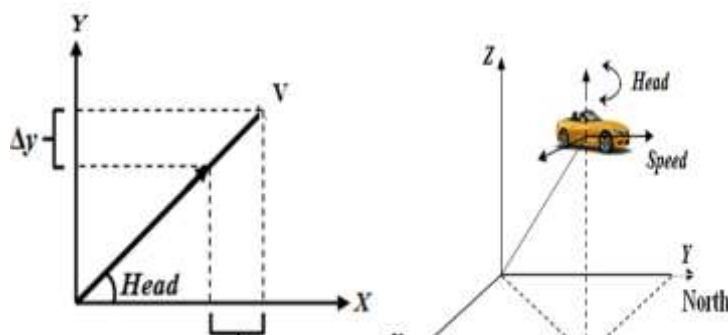


Figure 1-The directional head of the robotic car.

### Control Parameters

The change of the control parameters causes specific changes in the guidance parameters. Whereas, each guidance parameter has a direct effect on the corresponding control parameter. Therefore, the control tools can guide the car to specific guidance states according to the linear proportional command model as follows[12].:

$$\Delta C_i = k_{2i} \Delta G_i \quad \dots (4)$$

where  $\Delta C_i$  and  $\Delta G_i$  are the deflections of control and guidance parameters,  $k_{2i}$  is the proportional factor, and  $i$  is an index takes the values (1 or 2), it specifies the control and guidance parameters according to Table-1.

Table 1-Control and guidance parameters.

$i$	Control parameters	Guidance parameters
1	Throttle	RPM
2	Steering	Rotation

### Proposed Guidance Method

The generic structure of the proposed obstacle avoidance robotic system is explain in Figure-2. The suggested method contains three main stages; they are *Setting Stage*, *Control Module*, and *Obstacle Avoidance Module*. The setting stage is a preparing stage in which the initial values of the used

parameters are determined; these initial values are either determined by used sensors or determined by assigning useful initial values.

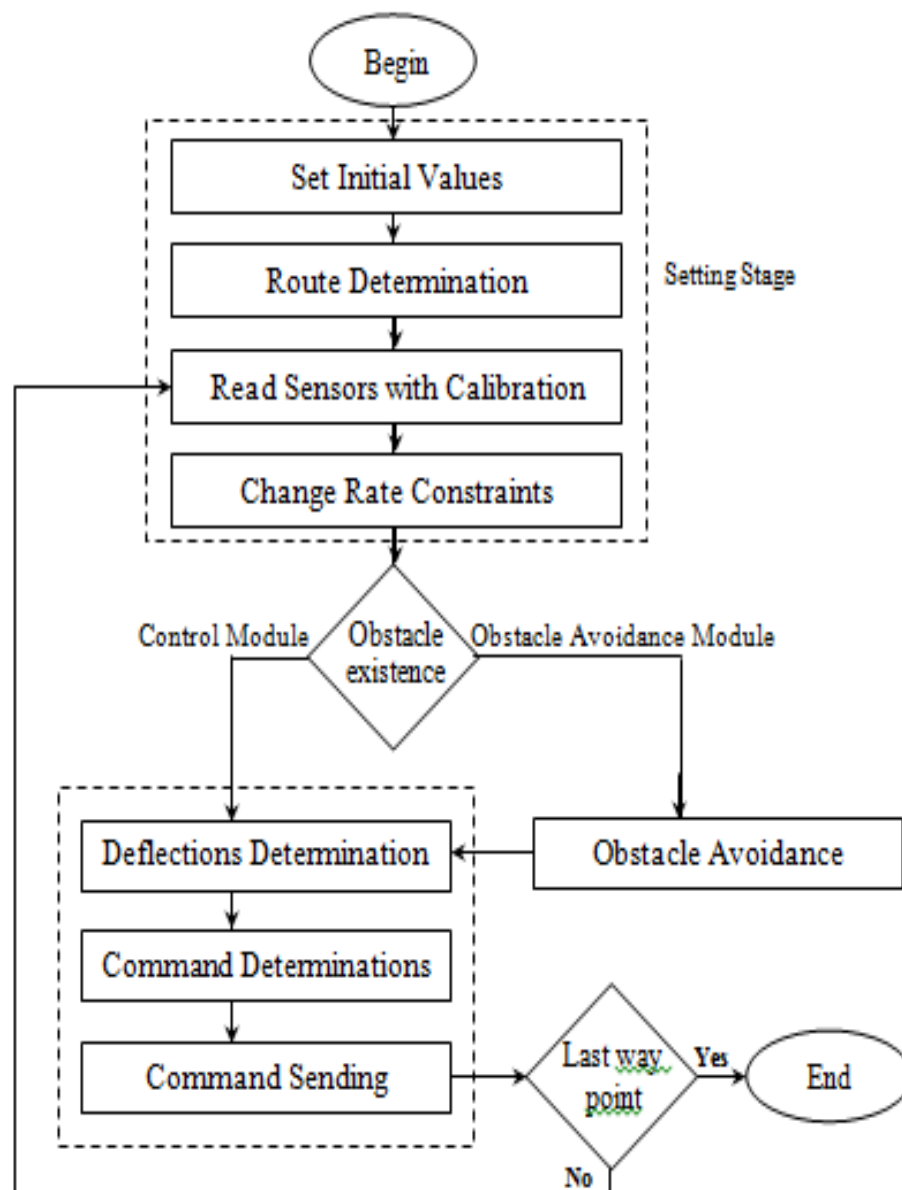


**Figure 2-**Flow chart of proposed control and obstacle avoidance method

Actually, condition parameters are sensed by the sensor, while the navigation and guidance parameters are set to be zeros. On the other hand, the controlling module includes a control system establishment, which is based on the concept of action reaction that mentioned before; it aims at controlling the auto guided car during its mission. The idea is implemented by introducing a specific action according to accounted determinations, and then the expected reaction will navigate the car toward the desired situation. Whereas, the obstacle avoidance stage is based on the feedback of the IR sensor that detect an obstacle on the path of the car and then suggest an effective method for dealing with obstacle that ahead the robotic car.

### **Route Determination**

During the guidance, the instantaneous values of the intended and actual values of the guidance and navigation parameters are displayed through two adjusted text boxes, while the control parameters are displayed on another text box. Also, the intended and actual head values are pointed on two text

boxes. While both the actual and intended routes are pointed as two trajectories drawn on the graphical map. The map carries information about the geographical features of the guidance region. This information besides the desired conditions are put in a dedicated *database* established for a certain guidance trip. The database has a set of records, each record includes the intended attitude of the car at certain route segment connecting a pair of successive way points. Table-2 shows an example of planned attitude registered as records in the database.

**Table 2**-Input database of an intended situations

Way Points	Position		Speed (m/s)	Radius of arrival (m)
	Longitude (degree)	Latitude (degree)		
1	$2 \times 91$	$2 \times 112$	0.1	0.25
2	$5 \times 91$	$4 \times 112$	0.125	0.25
3	$6 \times 91$	$8 \times 112$	0.10	0.25
4	$12 \times 91$	$3 \times 112$	0.13	0.25

The last column in Table-2 helps the navigator to switch to the next way point. The process of switching is done by comparing the distance  $RemDis$  between the current position  $(x_{Act}, y_{Act})$  on the actual route and the target way point  $(x_2, y_2)$  with the radius of arrival of the target way point. If  $RemDis$  is less than the radius of arrival then the car is considered arrived to the end of current route segment (reach the area of the target way point). Therefore, the auto-navigator should switch with the next way point within the planned route. The pointed circle, shown in Figure-3, represents the area of the arrival of the way point, and its radius is the radius of arrival of that way point.

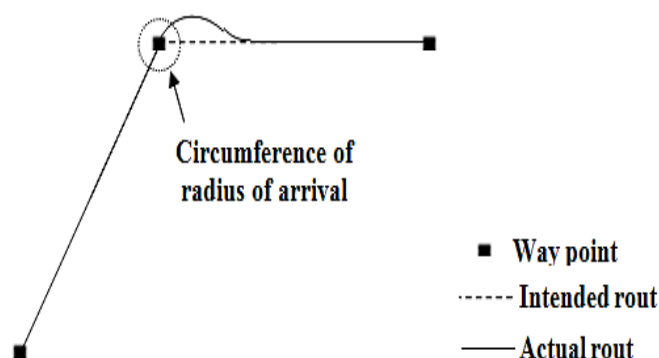


**Figure 3**-The radius of arrival

### acle Avoidance Module

This module is activated only when the controller detects an obstacle along the actual path. It depends on the feedback of both IR sensor and visual sensor. The IR sensor tells the distance between the car and the obstacle, while the visual sensor tells the size of the obstacle and its motion direction. Actually, the visual sensor is a simple camera put on the robotic car, in which the dark obstacle in bright environment is appeared in the captured digital images such that, it is easy to convert the image into binary form, where the obstacle appeared in black color and other detail appear in white. This enables to estimate the size of the obstacle by transforming the length of the obstacle ( $L_{img}$ ) in the image that measured by pixel into true length ( $L_{Obs}$ ) that is measured by meters when determining the width of the captured image ( $W_{img}$ ) and the scale factor ( $S_F$ ) of transforming the transverse image coordinate (which is the same as width of the image) into the real world coordinate (which is the width of region included in the image:  $W_{Real}$ ) which is related to the field of view (FOV) of the used camera as shown in Figure -4, as follows[13].:

$$L_{Obs} = \frac{L_{Img}}{W_{Img}} \times S_F \quad \dots (5)$$

$$S_F = \frac{W_{Real}}{W_{Img}} \quad \dots (6)$$

Also, the successive image captured by the visual sensor enables to determine the direction of the obstacle motion, the two differences between two successive images showed that the direction of the obstacle is biased toward the right or the left of the car. The changes that happen in the two captured images are detected by computing the absolute difference between the current image and the next one. The result of the difference is an image which contains expanded dark region except the region of the moving obstacle that appeared bright.

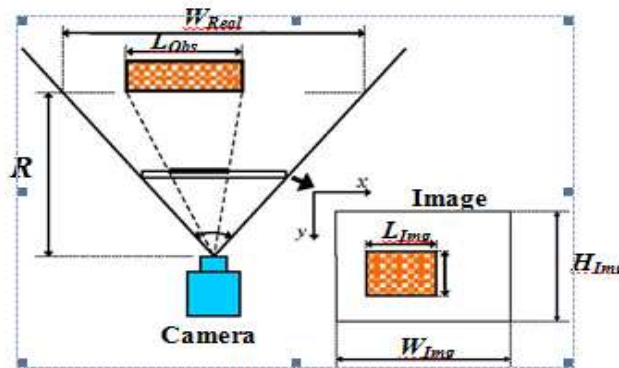


Figure 4-Obstacle information given by visual sensor

Figure 5-shows the difference image, in which the dark regions refer to the fact that the difference between the corresponding regions in the two images is very small approach to zero, due to the same background appearing on the two frames whereas the difference of the region in which the obstacle moves, is greater in comparison with the dark region. Such regions appeared relatively lighter.

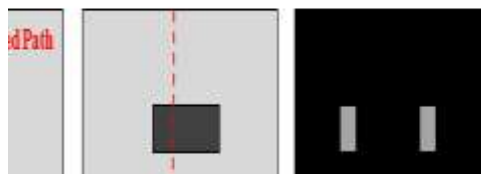


Figure 5-Difference image computation.

The direction of obstacle motion is determined by computing the vector of pixels weight ( $V_w$ ) two times, where  $V_w$  is one dimensional array of length equal to the width of image, each element in the  $V_w$  represents the average value of the pixels in the difference image as Figure-6 shows.

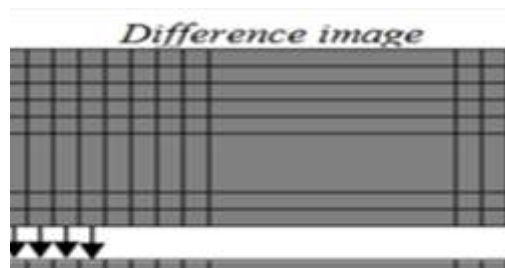


Figure 6-computation of  $V_w$ .

The behaviors of such curves contain two characteristics peaks as shown in Figure-7, each peak refers to the location of the obstacle in one image.



**Figure 7-** $V_w$  versus width of the image.

The direction of obstacle motion ( $D_o$ ; right or left) is determined using localization ( $L_p$ ) of these peaks, whereas the speed of the obstacle ( $S_{Obs}$ ) is determined by dividing the average absolute differences of the two peaks localizations in the two images by the average time ( $2s$ ) which requires to move the obstacle from the position (1) in the first image up to position (2) in the second image as shown in Figure-8.

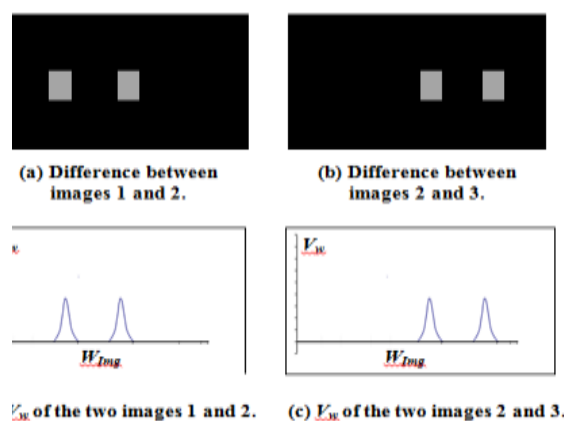


**Figure 8-**Difference image computation

Thus, the direction and speed of the obstacle are determined as follows:

If  $L_{p,1} > L_{p,2}$  then the obstacle directed toward left

ElseIf  $L_{p,2} > L_{p,1}$  then the obstacle directed toward right: Otherwise the obstacle is stopped

$$S_{Obs} = \frac{\sum_{i=1}^2 |L_{p,i+1} - L_{p,i}|}{2} \quad \dots (7)$$

In such case, the controller creates a transient way point at location in front of the obstacle and far away from the obstacle edge by a safety distance ( $D_s$ ), and then switches the control process to this point. Thus, the transient point will be the new destination that the controller drives the car into. Accordingly, the controlling events may be changed according to the new change as follows: 1-if the obstacle is directed toward the right of the car, then the transient way point will be at the left. 2.while the car may be speeded down when the obstacle moves in slow speed.

3. otherwise the car remains in its same speed when the obstacle moves in relatively higher speed and the remaining distance between the car and the obstacle is enough make the required change.

In this research, it is assumed that the obstacle moves horizontally in the direction that is perpendicular to the attended path. Therefore, the IR sensor feeds a binary reading: True refers to the existence of the obstacle while False refers to the absence of obstacle. Actually, false IR sensing may also refer to

absence of the obstacle along the sensing range of the IR sensor, where the IR sensing may be changed into true when the car becomes closer to the obstacle and the obstacle being in the range of the sensor. In case of true IR sensing, the IR sensor feeds the distance (R) between the car and obstacle.

### Results and Discussion

The data Table of the guidance parameters, shown in Table-3, is fed to the auto-navigation system as navigation situations. Table (4) presents the guidance specifications that could be setup for calibrating and ensuring smooth behavior in the change of the guidance parameters. These specifications are usually determined depending on the car capabilities.

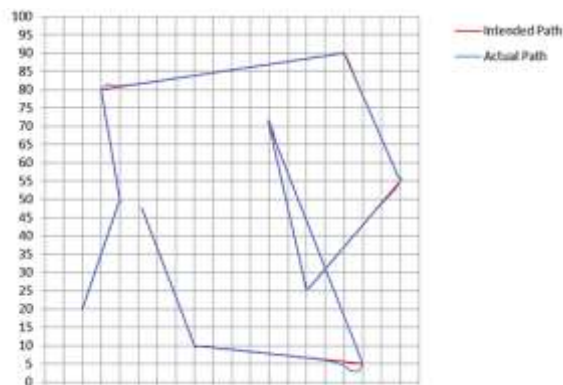
**Table 3-**Data Table of the guidance trip.

Way point	Position		Speed (km/h)	Radius of arrival (m)
	Longitude (km)	Latitude (km)		
1	10×91	20×112	20	5
2	20×91	4×112	80	5
3	15×91	5×112	40	5
4	80×91	1.5×112	70	5
5	25×91	2.5×112	60	5
6	70×91	3.5×112	30	5
7	60×91	7×112	100	5
8	85×91	5×112	90	5
9	40×91	10×112	70	5
10	27×91	47×112	80	5

**Table 4-**Specifications of the considered parameters

Parameter	Min. value	Max. value	Max. change
Speed (km/h)	0	100	1
RPM (rpm)	1000	8000	70
Throttle	1000	8000	70
Turn Degree)	-180	180	3.6
Rotation Degree)	-45	45	0.9
Steering Degree)	-90	90	1.8
Head (Degree)	-180	180	3.6

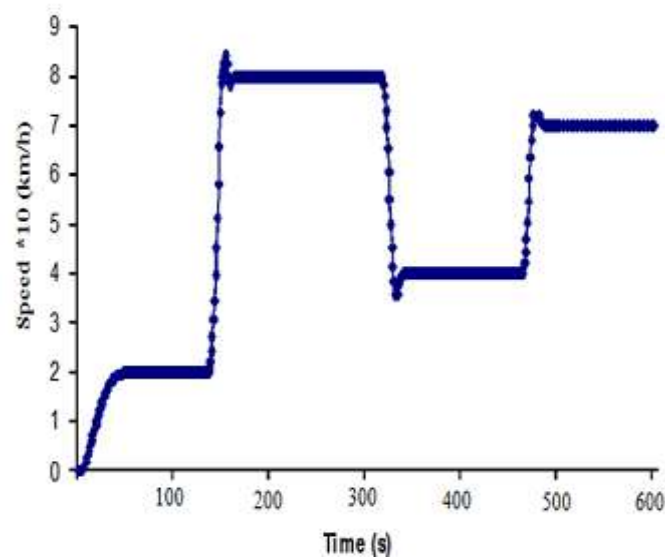
In the simulation, the response coefficients is set to be one, the radius of arrival is set 5 m, and the maximum change of each parameter is equal to one percent (1%) of the range of any parameter, this percentage is called Fraction factor since it may be useful to control the dynamic response, it has been noticed that the setting of the fraction factor at 1% provides least overshoot and more stability for the navigation and guidance parameters. Figure-9 shows the actual and intended route of the simulator.



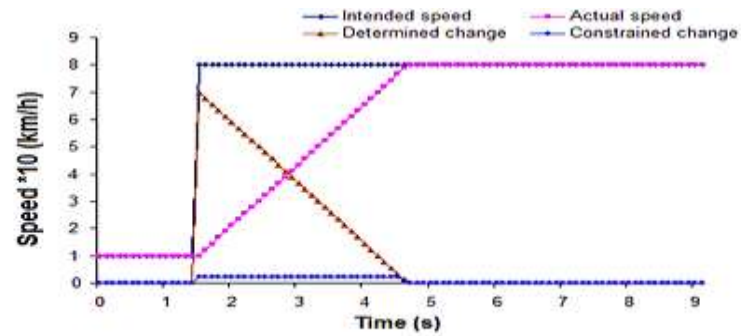
**Figure 9-**Intended and actual paths of the considered ten way points.

### Condition and Control Parameters Results

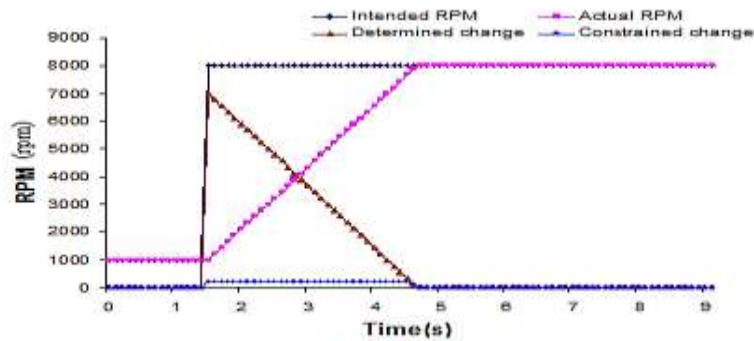
Experimentally, the behavior of the condition parameters against intended changes in the guidance or navigation parameters has been analyzed by adopting the changes in route segment toward the second way point given in Table-3. Firstly, one can consider just the speed condition parameter and note its behavior after switching to the second way point (i.e., this happens after passing through the first way point) that predetermined in the guidance plan, then the value of the intended speed will be 80 km/h and the actual speed became 20 km/h (is the intended speed of last route segment). The determined change of speed has been allowed to reach maximum positive value of the corresponding guidance parameter (maximum,  $IntRPM=60$ ) according to equation (3). The positive sign comes from the positive desired change of the speed (i.e., the simulator was positively accelerated) while the actual speed was still zero (i.e.,  $ActRPM=0$ ) since the guidance (at the way point switching instance) was still at level state. Therefore, the deflection of the RPM becomes a large positive value. Already, the deflection in the speed is restricted by the maximum amount of change in the speed, therefore, the current value of the actual change of the speed. This small change in the speed makes fewer changes in the throttle by an amount proportional to the amount of the attended deflection in the speed. Thus, the throttle that has a previous value equal to zero will change its state to be equal to 1, this has led to an increase in the RPM and then actual speed, and the simulator has shown positive accelerated behavior. As a result, the state of the speed was changing with an associative increase in the throttle. Figure-10 shows the behavior of the actual speed when the simulator follows the intended path given in the considered ten waypoints of Table-3. It is shown that the actual speed rise from the initial zero value up to the intended speed of value 20 km/h at about 40s, which is an acceptable acceleration for adopted type of robotic car. Then, the speed remains at the intended value until reaching the second way point where the speed is changed into the intended speed of 80 km/h and then other intended values of other way points. It is noticeable that the overshoot occurs when the speed becomes closer to the intended value in the two cases of speed up and speed down, it is of small value and it is quickly corrected.



**Figure 10**-Behavior of the simulator's speed through the considered ten way points



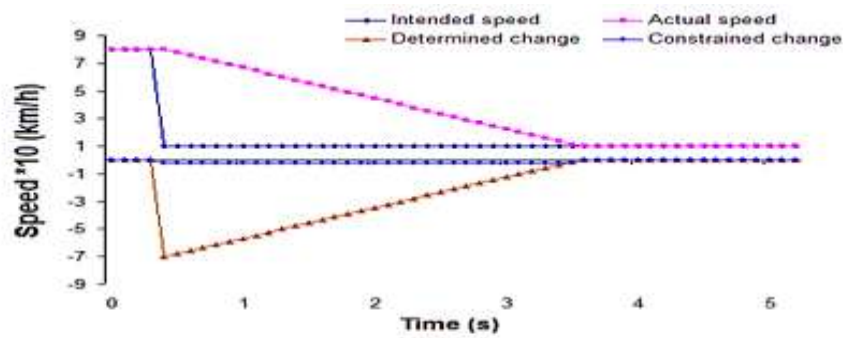
a. Speed behavior.



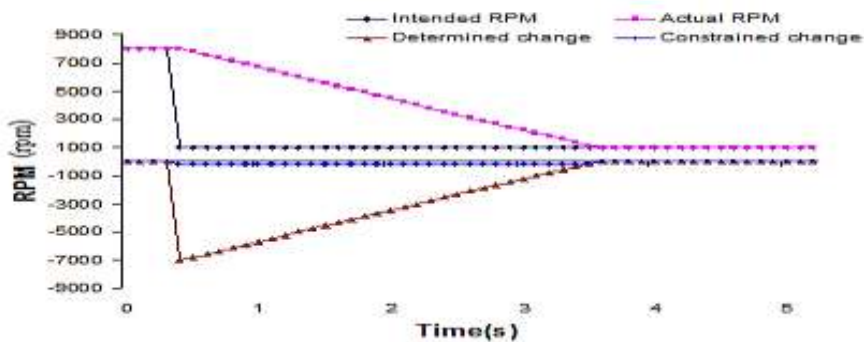
b. RPM behavior.

Figure 11-Simulated speed and RPM at speedup state..

Figures-(11-13) shows the behaviors of the actual and the intended speed besides their deflections and constrained deflection for one considered intended path segment. The behavior of the RPM and throttle associated with the intended speed variation are given below:

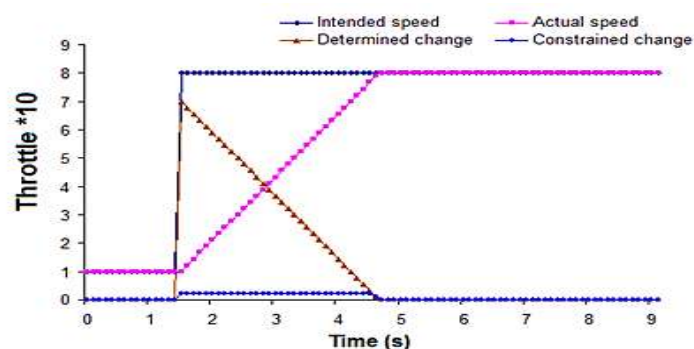


a. Speed behavior.

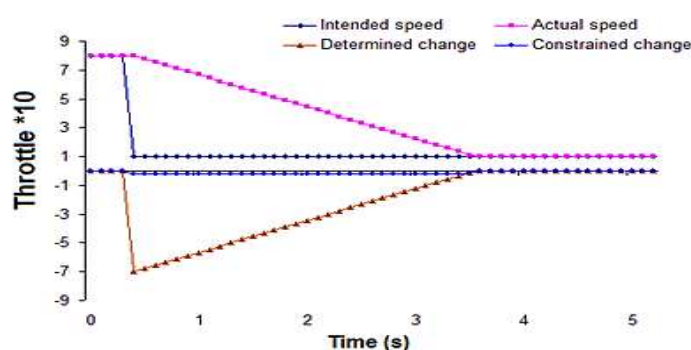


b. RPM behavior.

Figure 12-Simulated speed and RPM at slowdown state.



a. Throttle behavior at speed up situation.



b. Throttle behavior at speed down situation.

**Figure 13**-Simulated throttle behaviors at different situations.

At intervals of head changing; the intended steering remained constant along all the correction intervals, while the actual steering changed periodically toward the desired value due to the continuous correction. The deflection of the steering had reached the maximum value at first correction intervals (after the switching instance) and it was decreased gradually .

Since the intended turn is proportional to the deflection of the steering, its same behavior of change was similar to that for the deflection of the steering (i.e., it was gradually decreased). The actual turn that was in normal state (i.e., its angle equal to zero) was continually raised toward the intended. The deflection of the turn earned large value at the first correction intervals and then it decreased smoothly due to the decrease in the deflection of the steering. The positive turn deflection had caused the steering to move continuously toward the positive direction. These changes in steering status caused gradual increase in the steering that computed by the simulator. The predicted deflection of the turn was straight line as well as the determined deflection of the turn was greater than the amount of the maximum allowed change in the turn, for such cases it was clipped to be equal to the maximum allowable value. This led to make the simulator actual turn increased by a rate proportional to the maximum change of the turn. The deflection of the determined turn remained straight until it reaches the case where the deflection of the turn became less than the maximum allowed change in the turn, and then it was gradually decayed at each correction interval.

As a result, the deflection in the steering was decreased, the intended turn was decreased, and the actual turn was increased. At the same time, both the deflections in the steering and turn have been decreased sequentially due to continual correction in the steering. Also, the determined actual steering (by the simulator) was increased following the intended steering, till reaching the transient state.

The transient state occurs when the actual turn value reach a maximum allowed value, in such cases the deflection of the turn becomes zero. This state remains until the intended turn becomes equal or close to the actual turn, in this state the actual turn shows an intendment to reverse its behavior.

After the transient point, the correction of the steering is still continuing, the intended steering remains fixed as it was, the actual steering remains continually increase, and the deflection of the steering has decreased till reaching the value zero. On the other hand, the decrease in the turn

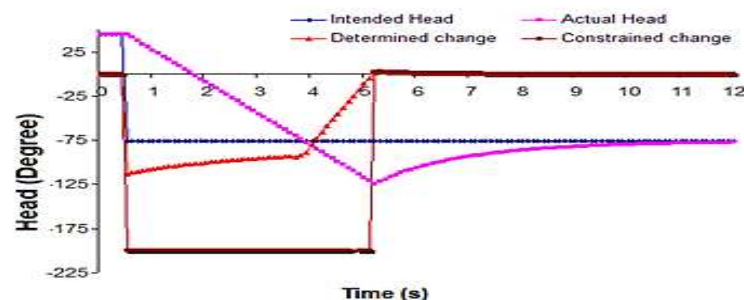
deflection continues and becomes a negative value because of the retreat of the intended turn from the actual turn, i.e. the intended turn becomes smaller than the actual one. The intervals characterized by the negative change of the turn led the steering decrease back to its normal state ( ), such state occurs when both the actual turn and the intended turn become zero. Also, one can notice that the change in the predicted deflection of the turn is little and it takes a long time to become zero.

Figures-(14 and 15) illustrate the corresponding behaviors of the guidance parameters due to the deflections that happened in the navigation parameters for different cases. The navigation parameters are also shown in these figures. An interesting behavior has been noticed; it is the uniform increase in the speed behavior, which is due to the uniform acceleration imposed by the simulator (car) during the simulation (guidance).

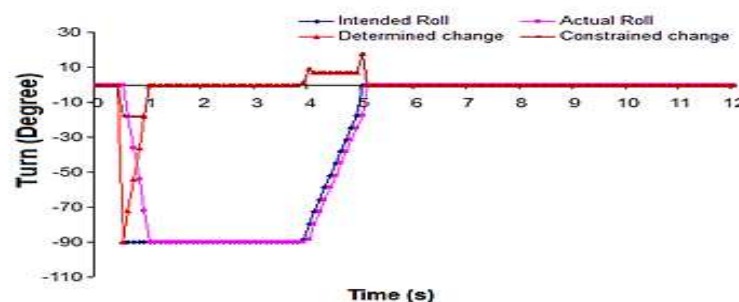
In the following paragraphs the behaviors of both the navigation and guidance parameters (except the speed and RPM) are described for the two cases; before and after the reversion state.

Before the transient state, the intended navigation parameter remained as it is along the time of corrections; the actual navigation parameter was gradually corrected toward the intended value. The changes in the navigation parameters behaved in inverse manner with the behavior of the actual navigation parameter. While the behaviors of the intended guidance parameters were similar to behaviors of the changes of the corresponding navigation parameters. The actual guidance parameters follow the intended, and the behavior of deflection of the guidance parameters (before the transient state) is linear as long as the determined deflection of the guidance parameters is greater than the amount of the maximum changes in the guidance parameters. The deflection in the guidance parameters decreases, and begins to decay slowly until it reaches zero at the transient state.

After the transient point, the change in guidance parameter continues in same way. The actual guidance parameter changes its course of change from increasing/decreasing or decreasing increasing (i.e., reverse its behavior).

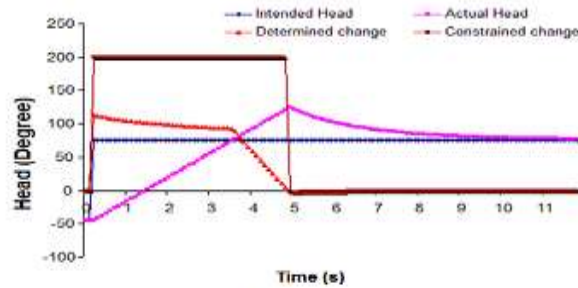


a. Head behavior.

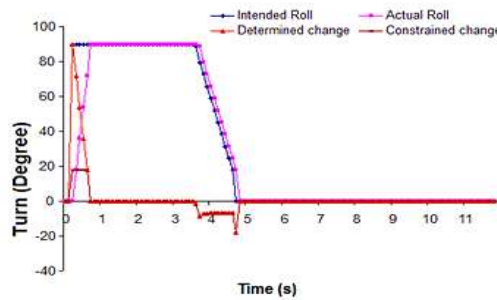


b. Turn behavior.

**Figure 14-** Simulated speed and RPM at slowdown state.



a. Head behavior.



b. Turn behavior.

Figure 15-Simulated head and turn at left turn.

**Control Result Analysis**

Figure-16 describes the behavior of the guidance parameters and its effect on the navigation parameters when the response coefficients are taken to be equal to one. The behaviors become faster when the corresponding response coefficients are taken greater than one, and they are slower when the response coefficient is taken less than one.

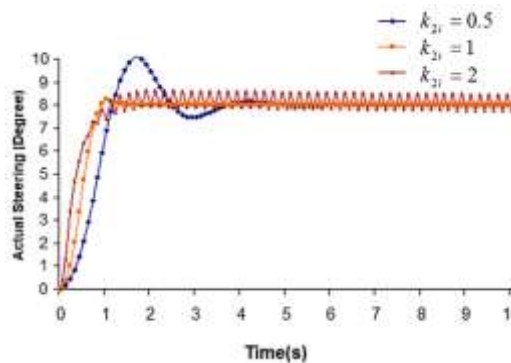
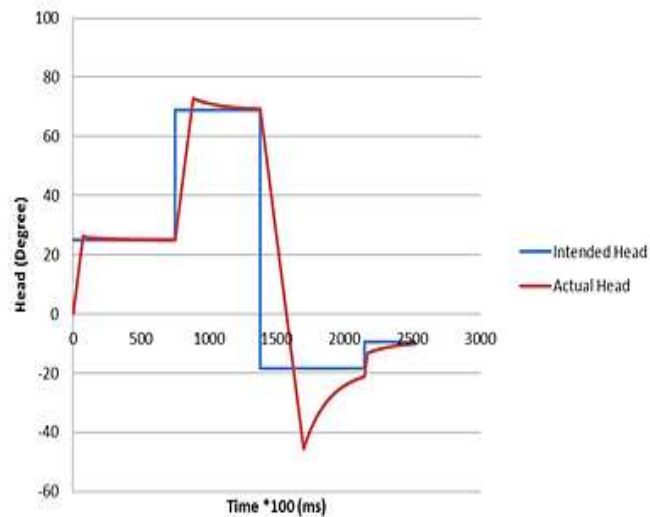


Figure 16-Simulated actual steering behavior for different values of  $k_{2i}$ .

**Obstacle Avoidance Result**

when facing an obstacle ahead, once the transient point that created to pass around the obstacle is found at the right of the simulator, while the second case includes a created transient point at the left of the obstacle, such case is achieved by changing the speed of the obstacle. These transient points are

found in a distance is greater than the length of the obstacle by an amount is equal to the assumed safety distance. It is shown that the simulator was able to change its direction toward the transient point effectively. When the simulator sense the existence of obstacle ahead, the intended path is changed toward the transient point, and then the actual path that follow the intended one is also redirected toward the transient point. This required changing the head of the simulator by an angle is proportional to the amount of deflecting the intended path toward the transient point as shown in Figure-(17 and 18).



**Figure 17-**Intended and actual head variation when switching with the transient point.

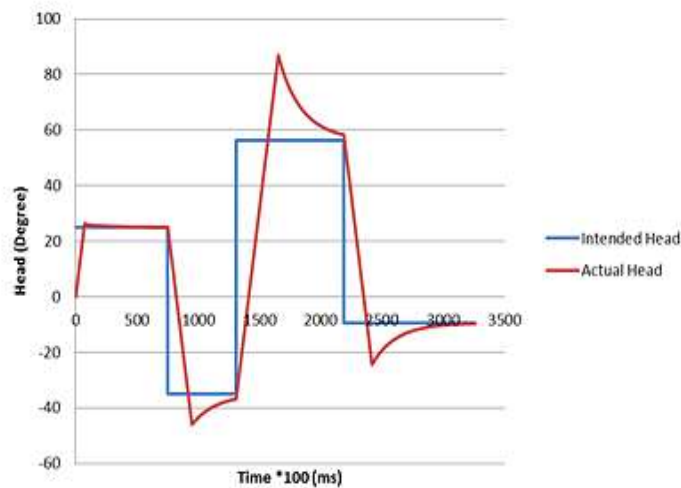


**Figure 18-**Intended and actual head variation when back to switch with the next way point.

At the moment when the simulator reaches the radius of arrival the transient point, the simulator back to switch with the next way point. Such that, the simulator was shown back to identify the original intended path. It is shown that the behavior of the simulator from the previous way point to the transient point is identical to that of the transient point to the next way point, this refers to the stability of the simulator against the intended head variation. It is noticeable that the head correction when the simulator directed to the right direction consumes a time is longer than that of the left deflection. This is due to the position of the obstacle was closer to the simulator at the case of the right deflection. This indicates the correct behavior of the simulator against the faced obstacle, and proves the correct way of the assumption and solution of the present research.

## Conclusions

The implementation of obstacle avoidance problem was successful at different simulated situations of robotic vehicle, this ensure the efficiency of the proposed obstacle avoidance method depending on the used guidance model. Different experimental guidance tests show that the best value of the Fraction factor is 0.01, which is useful to control the dynamic response of the controller that providing least overshoot and more stability for the navigation and guidance parameters. The deflections earned large value at the first correction intervals and then it decreased smoothly. The behavior of the deflection is linear as long as the determined deflection is greater than the amount of the maximum changes, which is decreasing gradually till reaching a zero value at the transient state. The rate of change of the actual steering depends directly upon the actual speed. The overshoot usually occurs when a large deflection in the head of a turn associated with high speed car is needed to occur. The safety distance is proportional to the size of the faced obstacle. The simulator is able to change its direction toward the transient point effectively when facing obstacle ahead.

## References

1. Wail Gueaieb, Md. Suruz Miah, **2008**. "An Intelligent Mobile Robot Navigation Technique Using RFID Technology", *IEEE Transactions On Instrumentation And Measurement*, **57**(9), September 2008.
2. Frank L.Lewis, Darren M.Dawson, Chaouki T.Abdallah **2004**. "Robot Manipulator Control Theory and Practice". Second Edition, ISBN: 0-8247-4072-6 Copyright © 2004 by Marcel Dekker, Inc.
3. Siegwart, Roland, Illah Reza Nourbakhsh, and Davide Scaramuzza, **2011**. "Introduction to autonomous mobile robots", MIT press.
4. Desouza, G. and Kak, A. **2002**. "Vision for mobile robot navigation: A survey", *IEEE Transactions on Pattern Analysis and Machine Intelligence*, **24**: 237–267. 2002.
5. Darius Burscka, Stephen Lee and Gregory Hager, **2002**. "Stereo- Based Obstacle Avoidance in Indoor Environments with Active Sensor Re-Calibration", proceeding of the 2002 IEEE International Conference on Robotics & Automation, Washington, DC. May 2002.
6. Kyuhyong You, **2008**. "Autonomous Navigation and Obstacle Avoidance Vehicle", proceeding in EEL 5666: Intelligent Machines Design Laboratory Spring 1st Written Report, University of Florida.
7. Taichi Yamada, Yeow Li Sa and Akihisa Ohya, **2013**. " Moving Obstacle Avoidance for Mobile Robot Moving on Designated Path", 10th International Conference on Ubiquitous Robots and Ambient Intelligence (URAI) Ramada Plaza Jeju Hotel, Jeju, Korea /October 31-November 2.
8. Anish Pandey, **2017**. "Mobile Robot Navigation and Obstacle Avoidance Techniques: A Review ", *International Robotics & Automation Journal*, **2**(3), 25 May 2017.
9. Hofmann-Wellenhof, Bernhard, Klaus Legat, and Manfred Wieser. **2011**. Navigation: principles of positioning and guidance. *Springer Science & Business Media*, 2011.
10. Kleppner, Daniel, and Robert Kolenkow. **2013**. *An introduction to mechanics*. Cambridge University Press, 2013.
11. Junkins, John L., and Hanspeter Schaub. **2009**. *Analytical mechanics of space systems*. American Institute of Aeronautics and Astronautics, 2009.
12. Faraway, Julian J. **2016**. *Extending the linear model with R: generalized linear, mixed effects and nonparametric regression models*. **124**. CRC press, 2016.
13. Zhang, Hong, and James P. Ostrowski. **2002**. "Visual motion planning for mobile robots." *IEEE Transactions on Robotics and Automation*, **18**(2): 199-208.